

Towards Safe Reinforcement Learning Using NMPC and Policy Gradients: Part I - Stochastic case

Sébastien Gros, Mario Zanon

Abstract—We present a methodology to deploy the stochastic policy gradient method, using actor-critic techniques, when the optimal policy is approximated using a parametric optimization problem, allowing one to enforce safety via hard constraints. For continuous input spaces, imposing safety restrictions on the stochastic policy can make the sampling and evaluation of its density difficult. This paper proposes a computationally effective approach to solve that issue. We will focus on policy approximations based on robust Nonlinear Model Predictive Control (NMPC), where safety can be treated explicitly. For the sake of brevity, we will detail safe policies in the robust linear MPC context only. The extension to the nonlinear case is possible but more complex. We will additionally present a technique to maintain the system safety throughout the learning process in the context of robust linear MPC. This paper has a companion paper treating the deterministic policy gradient case.

Index Terms—Safe Reinforcement Learning, robust Model Predictive Control, stochastic policy gradient, interior-point method.

I. INTRODUCTION

Reinforcement Learning (RL) is a powerful tool for tackling Markov Decision Processes (MDP) without depending on a detailed model of the probability distributions underlying the state transitions. Indeed, most RL methods rely purely on observed state transitions, and realizations of the stage cost $L(s, a) \in \mathbb{R}$ assigning a performance to each state-input pair s, a (the inputs are often labelled actions in the RL community). RL methods seek to increase the closed-loop performance of the control policy deployed on the MDP as observations are collected. RL has drawn an increasingly large attention thanks to its accomplishments, such as, e.g., making it possible for robots to learn to walk or fly without supervision [20], [1].

Most RL methods are based on learning the optimal control policy for the real system either directly, or indirectly. Indirect methods typically rely on learning a good approximation of the optimal action-value function underlying the MDP. The optimal policy is then indirectly obtained as the minimizer of the value-function approximation over the inputs a . Direct RL methods, based on policy gradients, seek to adjust the parameters θ of a given policy π_θ such that it yields the best closed-loop performance when deployed on the real system. An attractive advantage of direct RL methods over indirect ones is that they are based on formal necessary conditions of optimality for the closed-loop performance of π_θ , and therefore asymptotically (for a large enough data set) guarantee the (possibly local) optimality of the parameters θ [19], [17].

RL methods often rely on Deep Neural Networks (DNN) to carry the policy approximation π_θ . While effective in practice, control policies based on DNNs provide limited opportunities for formal verifications of the resulting closed-loop behavior, and for imposing hard constraints on the evolution of the state of the real system. The development of safe RL methods, which aims at tackling this issue, is currently an open field or research [12].

In this paper, we investigate the use of constrained parametric optimization problems to carry the policy approximation. The aim is to impose safety by means of hard constraints in the optimization problem. In that context, we investigate some straightforward options to build a safe stochastic policy, and discuss their shortcomings when using the stochastic policy gradient method. We then present an alternative approach, and propose tools to make its deployment computationally efficient, using the primal-dual interior-point method and techniques from parametric Nonlinear Programming.

Robust Nonlinear Model Predictive Control (NMPC) is arguably an ideal candidate for forming the constrained optimization problem supporting the policy approximation. Robust NMPC techniques provide safety guarantees on the closed-loop behavior of the system by explicitly accounting for the presence of (possibly stochastic) disturbances and model inaccuracies. A rich theoretical framework is available on the topic [14]. The policy parameters θ then appear as parameters in the NMPC model(s), cost function and constraints. Updates in the policy parameters θ are driven by the stochastic policy gradient method, increasing the NMPC closed-loop performance, and constrained by the requirement that the NMPC model inaccuracies are adequately accounted for in forming the robust NMPC scheme. For the sake of brevity and simplicity, we will detail these questions in the specific linear robust MPC case. The extension to the nonlinear case is arguably possible, but more complex.

This paper has a companion paper [11] treating the same problem in the context of the deterministic policy gradient approach. The two papers share some material and use similar techniques, but present very different theories. Additionally [21] discusses the management of safety in RL using tube-based techniques.

The paper is structured as follows. Section II provides some background material. Section III details the safe deterministic policy we use to build up the stochastic policy. Section IV investigates several options to build safe stochastic policies from the deterministic policy approximation, discusses their shortcomings and proposes a computationally efficient alternative based on disturbed parametric NLPs. Section V presents numerical tools for an efficient deployment of the stochastic

Sébastien Gros is with the Department of Cybernetic, NTNU, Norway.

Mario Zanon is with the IMT School for Advanced Studies Lucca, Lucca 55100, Italy.

policy gradient approach for the latter approach, using the primal-dual interior-point method and tools from parametric Nonlinear Programming. Section VI discusses a technique to ensure safety throughout the learning process, in the context of robust linear MPC. Section VII proposes an example of simulation using the principles developed in this paper.

II. BACKGROUND ON MARKOV DECISION PROCESSES

In the following, we will consider that the dynamics of the real system are described as a Markov Chain, with state transitions having the underlying conditional probability density:

$$\mathbb{P}[\mathbf{s}_+ | \mathbf{s}, \mathbf{a}] \quad (1)$$

denoting the probability density of the state transition from the state-input pair $\mathbf{s} \in \mathbb{R}^n$, $\mathbf{a} \in \mathbb{R}^{n_a}$ to a new state $\mathbf{s}_+ \in \mathbb{R}^n$. We will furthermore consider (possibly) stochastic policies π , taking the form of probability densities:

$$\pi[\mathbf{a} | \mathbf{s}] \quad (2)$$

denoting the probability density of selecting a given input \mathbf{a} when the system is in a given state \mathbf{s} . We should note here that a deterministic policy

$$\mathbf{a} = \pi(\mathbf{s}) \quad (3)$$

can always be cast as a stochastic policy (2) by defining:

$$\pi[\mathbf{a} | \mathbf{s}] = \delta(\mathbf{a} - \pi(\mathbf{s})) \quad (4)$$

where δ is the Dirac function. Let us then consider the distribution of the Markov Chain resulting from the state transition (1) and policy (2):

$$\mathbb{P}[\mathbf{s}_k | \pi] = \int \prod_{i=0}^{k-1} \mathbb{P}[\mathbf{s}_{i+1} | \mathbf{s}_i, \mathbf{u}] \mathbb{P}[\mathbf{s}_0] \pi[\mathbf{a}_i | \mathbf{s}_i] \quad (5)$$

$$d\mathbf{s}_0, \dots, \mathbf{s}_{k-1} d\mathbf{a}_0, \dots, \mathbf{a}_{k-1}$$

where $\mathbb{P}[\mathbf{s}_0]$ denotes the probability distribution of the initial conditions \mathbf{s}_0 of the MDP. We can then define the discounted expected value under policy π , which reads as:

$$\mathbb{E}_\pi[\zeta(\mathbf{s}, \mathbf{a})] = \sum_{k=0}^{\infty} \int \gamma^k \zeta(\mathbf{s}_k, \mathbf{a}_k) \mathbb{P}[\mathbf{s}_k | \pi] \pi[\mathbf{a}_k | \mathbf{s}_k] d\mathbf{s}_k d\mathbf{a}_k \quad (6)$$

for any function ζ . This definition can be easily extended for functions over state transitions, i.e. $\zeta(\mathbf{s}_+, \mathbf{s}, \mathbf{a})$. In the following we will assume the local stability of the MDP under the selected policies. More specifically, we assume that π is such that:

$$\lim_{\tilde{\pi} \rightarrow \pi} \mathbb{E}_{\tilde{\pi}}[\zeta] = \mathbb{E}_\pi[\zeta], \quad (7)$$

where the limit is taken in the sense of almost everywhere, and for any bounded function ζ such that both sides of the equality are finite. Assumption (7) will allow us to draw equivalences between a policy and disturbances of that policy, which will be required in the RL context.

For a given stage cost function $L(\mathbf{x}, \mathbf{u})$ and a discount factor $\gamma \in [0, 1]$, the performance of policy π is given by the discounted cost:

$$J(\pi) = \mathbb{E}_\pi[L] \quad (8)$$

The optimal policy associated to the MDP defined by the state transition (1), the stage cost L and the discount factor γ is then given by:

$$\pi_\star = \arg \min_{\pi} J(\pi) \quad (9)$$

It should be useful to underline here that, while (9) may have several (global) solutions, any fully observable MDP admits a deterministic policy π_\star among its solutions. The value function associated to a given policy π is given by [4], [6], [3]:

$$V_\pi(\mathbf{s}) = \mathbb{E}_{\mathbf{a} \sim \pi[\cdot | \mathbf{s}]} [L(\mathbf{s}, \mathbf{a}) + \gamma \mathbb{E}[V_\pi(\mathbf{s}_+) | \mathbf{s}, \mathbf{a}]], \quad (10)$$

where the internal expected value in (10) is taken over state transitions (1).

A. Stochastic policy gradient

In most cases, the optimal policy π_\star cannot be computed. It is then useful to consider a stochastic approximations π_θ of the optimal policy, carried by a (possibly large) set of parameters θ . The optimal parameters θ_\star are then given by:

$$\theta_\star = \arg \min_{\theta} J(\pi_\theta) \quad (11)$$

The policy gradient $\nabla_\theta J(\pi_\theta)$ associated to the stochastic policy π_θ can be obtained using various actor-critic methods, such as e.g. [18], [19]:

$$\nabla_\theta J(\pi_\theta) = \mathbb{E}_{\pi_\theta} [\nabla_\theta \log \pi_\theta \delta_{\pi_\theta}^V], \quad (12)$$

where

$$\delta_{\pi_\theta}^V = L(\mathbf{s}, \mathbf{a}) + \gamma V_{\pi_\theta}(\mathbf{s}_+) - V_{\pi_\theta}(\mathbf{s}) \quad (13)$$

The value function V_{π_θ} in (13) is formally given by (10), but typically approximated via a parametrized value function approximation and computed via Temporal-Difference (TD) techniques or Monte-Carlo techniques [18]. Note that is is fairly common in RL to generate the stochastic policy π_θ as a disturbed version of a deterministic policy π_θ by, e.g., adding a simple stochastic disturbance to π_θ .

In order to deploy the stochastic policy, π_θ needs to be sampled, to produce realizations of the inputs \mathbf{a} to be deployed on the system. Moreover, in order to compute the policy gradient, evaluations of the gradient of the policy score function:

$$\nabla_\theta \log \pi_\theta = \pi_\theta^{-1} \nabla_\theta \pi_\theta \quad (14)$$

are required in computing (12).

B. Safe set

In the following, we will assume the existence of a (possibly) state-dependent *safe set* labelled $\mathbb{S}(\mathbf{s}) \subseteq \mathbb{R}^{n_a}$, subset of the input space. The notion of safe set will be used here in the sense that any input selected such that $\mathbf{a} \in \mathbb{S}(\mathbf{s})$ yields safe future trajectories with a unitary probability. The construction of the safe set is not the object of this paper. However, we can nonetheless propose some pointer to how such a set is constructed in practice.

Let us consider the constraints $\mathbf{h}_s(\mathbf{s}, \mathbf{a}) \leq 0$ describing at any given future time i the subset of the state-input space deemed feasible and safe. Constraints \mathbf{h} can include pure state constraints, describing the safe states, pure input constraints, describing typically actuators limitations, and mixed constraints, where the states and inputs are mixed. For the sake of simplicity, we will assume in the following that \mathbf{h}_s is convex.

A common approach to build practical or inner approximations of the safe set $\mathbb{S}(\mathbf{s})$ is via verifying the safety of an input \mathbf{a} explicitly over a finite horizon via predictive control techniques. This verification is based on forming the support of the Markov Process distribution over time, starting from a given state-input pair \mathbf{s}, \mathbf{a} . Consider the set $\mathbf{X}_+(\mathbf{s}, \mathbf{a})$, support of the state transition (1),

$$\mathbf{X}_+(\mathbf{s}, \mathbf{a}) = \{ \mathbf{s}_+ \mid \mathbb{P}[\mathbf{s}_+ | \mathbf{s}, \mathbf{a}] > 0 \} \quad (15)$$

Labelling $\mathbf{X}_k(\mathbf{s}, \mathbf{a}, \pi^s)$ the support of the state of the Markov Process at time k , starting from \mathbf{s}, \mathbf{a} and evolving under policy π^s , the set \mathbf{X}_k is then given by the recursion:

$$\mathbf{X}_k(\mathbf{s}, \mathbf{a}, \pi^s) = \mathbf{X}_+(\mathbf{X}_{k-1}, \pi^s(\mathbf{X}_{k-1})), \quad (16)$$

with the boundary condition $\mathbf{X}_1 = \mathbf{X}_+(\mathbf{s}, \mathbf{a})$. An input \mathbf{a} is in the safe set $\mathbb{S}(\mathbf{s})$ if $\mathbf{h}_s(\mathbf{s}, \mathbf{a}) \leq 0$ and if there exist a deterministic policy π^s such that

$$\mathbf{h}_s(\mathbf{s}_k, \pi^s(\mathbf{s}_k)) \leq 0, \quad \forall \mathbf{s}_k \in \mathbf{X}_k(\mathbf{s}, \mathbf{a}, \pi^s), \quad (17)$$

for all $k \geq 1$. This verification is typically performed in practice via tube-based approaches, polynomial chaos, or direct approximations of the set \mathbf{X}_k via e.g. ellipsoids or polytopes. In that context, policy π^s is typically selected a priori to stabilize the system dynamics, and possibly optimized to minimize the size of the sets \mathbf{X}_k .

C. Safe stochastic policy

In this paper, we will consider safe, stochastic policies π_θ , which we will label

$$\pi_\theta[\mathbf{a} | \mathbf{s}] \quad (18)$$

We will build π_θ from a deterministic policy π_θ based on a constrained optimization scheme such that the support of π_θ is limited to the safe set $\mathbb{S}(\mathbf{s})$, i.e. such that

$$\mathbb{P}[\mathbf{a} \notin \mathbb{S}(\mathbf{s}) | \mathbf{a} \sim \pi_\theta[\mathbf{a} | \mathbf{s}]] = 0 \quad (19)$$

Unfortunately, when the support of the stochastic policy π_θ must be restricted within the given, possibly non-trivial safe set $\mathbb{S}(\mathbf{s})$, it is not always straightforward to build a stochastic

policy π_θ that is at the same time inexpensive to sample from and to evaluate.

There are clearly several approaches to generate random inputs that are in the safe set $\mathbb{S}(\mathbf{s})$ with unitary probability, but we will focus here on techniques that require a limited amount of computations, so as to make them real-time feasible.

III. OPTIMIZATION-BASED SAFE POLICY

In this paper, we will consider parametrized deterministic policies $\pi_\theta \approx \pi_*$ based on parametric optimization problems subject to safe stochastic disturbances. Before detailing the stochastic aspect, let us detail first the constrained optimization problems. We will consider parametrized deterministic policies π_θ based on parametric Nonlinear Programs (NLPs), and more specifically based on robust NMPC schemes. This approach is formally justified in [10]. More specifically, we will consider a policy approximation

$$\pi_\theta = \mathbf{u}_0^*(\mathbf{s}, \theta), \quad (20)$$

where $\mathbf{u}_0^*(\mathbf{s}, \theta)$ is the first n_a entries of $\mathbf{u}^*(\mathbf{s}, \theta)$ generated by the parametric NLP:

$$\mathbf{u}^*(\mathbf{s}, \theta) = \arg \min_{\mathbf{u}} \Phi(\mathbf{x}, \mathbf{u}, \theta) \quad (21a)$$

$$\text{s.t.} \quad \mathbf{f}(\mathbf{x}, \mathbf{u}, \mathbf{s}, \theta) = 0, \quad (21b)$$

$$\mathbf{h}(\mathbf{x}, \mathbf{u}, \theta) \leq 0. \quad (21c)$$

We will then consider that the safety requirement $\pi_\theta(\mathbf{s}) \in \mathbb{S}(\mathbf{s})$ is imposed via the constraints (21b)-(21c). A special case of (21) is an optimization scheme in the form:

$$\mathbf{u}_0^*(\mathbf{s}, \theta) = \arg \min_{\mathbf{u}_0} \Phi(\mathbf{s}, \mathbf{u}_0, \theta) \quad (22a)$$

$$\text{s.t.} \quad \mathbf{h}(\mathbf{s}, \mathbf{u}_0, \theta) \leq 0, \quad (22b)$$

where $\mathbf{h} \leq 0$ ought to ensure that $\pi_\theta(\mathbf{s}) = \mathbf{u}_0^*(\mathbf{s}, \theta) \in \mathbb{S}(\mathbf{s})$.

While most of the discussions in this paper will take place around the general formulation (21), a natural approach to formulate constraints (21b)-(21c) such that policy (20) is safe is to build (21) using robust (N)MPC techniques.

A. Policy approximation based on robust NMPC

The imposition of safety constraints can be treated via robust NMPC approaches. Robust NMPC can take different forms [14], all of which can be eventually cast in the form (21). One form of robust NMPC schemes is based on scenario trees [16], which take the form:

$$\mathbf{u}^*(\mathbf{s}, \theta) = \arg \min_{\mathbf{u}} \sum_{j=1}^{N_M} \left(V_j(\mathbf{x}_{j,N}, \theta) + \sum_{k=0}^{N-1} \ell_j(\mathbf{x}_{j,k}, \mathbf{u}_{j,k}, \theta) \right) \quad (23a)$$

$$\text{s.t.} \quad \mathbf{x}_{j,k+1} = \mathbf{F}_j(\mathbf{x}_{j,k}, \mathbf{u}_{j,k}, \theta), \quad \mathbf{x}_{j,0} = \mathbf{s}, \quad (23b)$$

$$\mathbf{h}^s(\mathbf{x}_{j,k}, \mathbf{u}_{j,k}, \theta) \leq 0, \quad (23c)$$

$$\mathbf{e}(\mathbf{x}_{j,N}, \theta) \leq 0, \quad (23d)$$

$$\mathbf{N}(\mathbf{u}) = 0, \quad (23e)$$

where \mathbf{F}_{1,\dots,N_M} are the N_M different models used to support the uncertainty, while \mathbf{F}_0 is a nominal model supporting the

NMPC scheme. Trajectories $\mathbf{x}_{j,k}$ and $\mathbf{u}_{j,k}$ for $j = 1, \dots, N_M$ are the different models trajectories and the associated inputs. Functions ℓ_{1,\dots,N_M} , V_{1,\dots,N_M} the (possibly different) stage costs and terminal costs applying to the different models. The *non-anticipativity constraints* (23e) support the scenario-tree structure. For a given state \mathbf{s} and parameters $\boldsymbol{\theta}$, the NMPC scheme (23) delivers the input profiles

$$\mathbf{u}_j^*(\mathbf{s}, \boldsymbol{\theta}) = \{\mathbf{u}_{j,0}^*(\mathbf{s}, \boldsymbol{\theta}), \dots, \mathbf{u}_{j,N}^*(\mathbf{s}, \boldsymbol{\theta})\}, \quad (24)$$

with $\mathbf{u}_{j,i}^*(\mathbf{s}, \boldsymbol{\theta}) \in \mathbb{R}^{n_a}$, and (23e) imposes

$$\mathbf{u}_0^*(\mathbf{s}, \boldsymbol{\theta}) := \mathbf{u}_{i,0}^*(\mathbf{s}, \boldsymbol{\theta}) = \mathbf{u}_{j,0}^*(\mathbf{s}, \boldsymbol{\theta}), \quad \forall i, j. \quad (25)$$

As a result, the NMPC scheme (23) generates a parametrized deterministic policy according to:

$$\pi_{\boldsymbol{\theta}}(\mathbf{s}) = \mathbf{u}_0^*(\mathbf{s}, \boldsymbol{\theta}) \in \mathbb{R}^{n_a}. \quad (26)$$

Policy π^s is implicitly deployed in (23) via the scenario tree. If the dispersion set \mathbf{X}_+ is known, the multiple models \mathbf{F}_{1,\dots,N_M} and terminal constraints (23d) can be chosen such that the robust NMPC scheme (23) delivers $\pi_{\boldsymbol{\theta}}(\mathbf{s}) \in \mathbb{S}(\mathbf{s})$. Unfortunately, this selection can be difficult in general. We turn next to the robust linear MPC case, where this construction is much simpler.

B. Safe robust linear MPC

Exhaustively discussing the construction of the safe scenario tree in (23) for a given dispersion set $\mathbf{X}_+(\mathbf{s}, \mathbf{a})$ is beyond the scope of this paper. The process can be fairly involved, and we refer to [16], [2] for detailed discussions. For the sake of brevity, we will focus on the linear MPC case, whereby the MPC models \mathbf{F}_{1,\dots,N_M} and policy π^s are linear.

Let us consider the following outer approximation of the dispersion set \mathbf{X}_+ :

$$\mathbf{X}_+(\mathbf{s}, \mathbf{a}) \subseteq \mathbf{F}_0(\mathbf{s}, \mathbf{a}, \boldsymbol{\theta}) + \mathbf{W}, \quad \forall \mathbf{s}, \mathbf{a} \quad (27)$$

where we use a linear nominal model \mathbf{F}_0 and a polytope \mathbf{W} of vertices \mathbf{W}^{1,\dots,N_M} that can be construed as the extrema of a finite-support process noise, and which can be part (or functions of) the MPC parameters $\boldsymbol{\theta}$. For the sake of simplicity, we assume that \mathbf{W} is independent of the state-input pair \mathbf{s}, \mathbf{a} . The models \mathbf{F}_{1,\dots,N_M} can then be built based using:

$$\mathbf{F}_i = \mathbf{F}_0 + \mathbf{W}^i, \quad i = 1 \dots N_M \quad (28)$$

and using the linear policy:

$$\pi^s(\mathbf{x}_{j,k}, \mathbf{u}_{0,k}, \mathbf{x}_{0,k}) = \mathbf{u}_{0,k} - K(\mathbf{x}_{j,k} - \mathbf{x}_{0,k}) \quad (29)$$

where matrix K can be part (or function of) the MPC parameters $\boldsymbol{\theta}$. One can then verify by simple induction that:

$$\mathbf{X}_k(\mathbf{s}, \mathbf{a}, \pi^s) \subseteq \text{Conv}(\mathbf{x}_{1,k}, \dots, \mathbf{x}_{N_M,k}), \quad (30)$$

for $k = 0, \dots, N+1$, where Conv is the convex hull of the set of points $\mathbf{x}_{1,k}, \dots, \mathbf{x}_{N_M,k}$ solution of the MPC scheme (23). The terminal constraints (23d) ought then be constructed as, e.g., via the Robust Positive Invariant set corresponding to π^s in order to establish safety beyond the MPC horizon. For \mathbf{h}^s convex, the MPC scheme (23) delivers safe inputs [14], [13].

Algorithm 1: Resampling

Input: State \mathbf{s} , conditional density $\varrho(\cdot|\cdot)$

Set *sample* = true

while *sample* **do**

 Draw $\mathbf{a} \sim \varrho(\cdot|\pi_{\boldsymbol{\theta}}^d(\mathbf{s}))$

if $\mathbf{a} \in \mathbb{S}(\mathbf{s})$ **then**

sample = false

return \mathbf{a}

When the dispersion set $\mathbf{X}_+(\mathbf{s}, \mathbf{a})$ can only be inferred from data, condition (27) arguably translates to [5]:

$$\mathbf{s}_{k+1} - \mathbf{F}_0(\mathbf{s}_k, \mathbf{a}_k, \boldsymbol{\theta}) \in \mathbf{W}, \quad \forall (\mathbf{s}_{k+1}, \mathbf{s}_k, \mathbf{a}_k) \in \mathcal{D}, \quad (31)$$

where \mathcal{D} is the set of $N_{\mathcal{D}}$ observed state transitions. Condition (31) translates into a sample-based condition on the admissible parameters $\boldsymbol{\theta}$, i.e., it specifies the parameters that are safe *with respect to the state transitions observed so far*. Condition (31) tests whether the points $\mathbf{s}_{k+1} - \mathbf{F}_0(\mathbf{s}_k, \mathbf{a}_k, \boldsymbol{\theta})$ are in the polytope \mathbf{W} , which can be easily translated into a set of algebraic constraints imposed on $\boldsymbol{\theta}$. This observation will be used in Section III-B to build a safe RL-based learning.

We ought to underline here that building \mathbf{F}_0 , \mathbf{W} based on (31) ensures the safety of the robust MPC scheme (23) only for an infinitely large, and sufficiently informative data set \mathcal{D} . In practice, using a finite data set entails that safety is ensured with a probability less than 1. The quantification of the probability of having a safe policy for a given, finite data set \mathcal{D} is beyond the scope of this paper, and is arguably best treated by means of the Information Field Theory [9]. The extension of the construction of a safe MPC presented in this section to the general NMPC case is theoretically feasible, but can be computationally intensive in practice. This aspect of the problem is beyond the scope of this paper.

IV. SAFE STOCHASTIC POLICIES

In this section, we discuss first two intuitively appealing methods to generate safe stochastic policies from $\pi_{\boldsymbol{\theta}}$, see Sections IV-A and IV-B, and detail their computational shortcomings in the context of NMPC-based RL discussed in this paper. We present then an alternative approach in Section IV-C.

A. Safe stochastic policy via resampling

Let us discuss first a very natural approach to generating a safe stochastic policy, based on re-generating a random input \mathbf{a} until it is in the safe set $\mathbb{S}(\mathbf{s})$. This can, e.g., be achieved by the trivial re-sampling Algorithm 1, where $\varrho(\cdot|\pi_{\boldsymbol{\theta}}(\mathbf{s}))$ is a probability density centred at $\pi_{\boldsymbol{\theta}}(\mathbf{s})$. One can, e.g., choose for $\varrho(\cdot|\cdot)$ a Normal distribution centered at $\pi_{\boldsymbol{\theta}}(\mathbf{s})$, i.e.,

$$\mathbf{a} \sim \mathcal{N}(\pi_{\boldsymbol{\theta}}(\mathbf{s}), \Sigma), \quad (32)$$

Verifying the condition $\mathbf{a} \in \mathbb{S}(\mathbf{s})$ can then be done via classic optimization techniques, where one verifies the feasibility of the constraints (21c) when selecting $\mathbf{u}_0 = \mathbf{a}$ in (21) according to the proposed \mathbf{a} .

One can verify that the resulting stochastic policy $\pi_\theta[\mathbf{a}|\mathbf{s}]$ takes the probability density:

$$\pi_\theta[\mathbf{a}|\mathbf{s}] = \frac{\varrho(\mathbf{a}|\pi_\theta(\mathbf{s}))}{\mu_\varrho(\mathbb{S}(\mathbf{s}))}, \quad (33)$$

where $\mu_\varrho(\mathbb{S}(\mathbf{s}))$ is the measure of density ϱ over $\mathbb{S}(\mathbf{s})$, i.e.,

$$\mu_\varrho(\mathbb{S}(\mathbf{s})) = \int_{\mathbb{S}(\mathbf{s})} \varrho(\mathbf{a}|\pi_\theta(\mathbf{s})) d\mathbf{a}. \quad (34)$$

We observe then that the gradient of the score function required in calculating (12) reads as:

$$\begin{aligned} \nabla_\theta \log \pi_\theta[\mathbf{a}|\mathbf{s}] &= \nabla_\theta \log \varrho(\mathbf{a}|\pi_\theta(\mathbf{s})) \\ &\quad - \nabla_\theta \log \mu_\varrho(\mathbb{S}(\mathbf{s})), \end{aligned} \quad (35)$$

such that

$$\nabla_\theta \log \mu_\varrho(\mathbb{S}(\mathbf{s})) = -\frac{\nabla_\theta \mu_\varrho(\mathbb{S}(\mathbf{s}))}{\mu_\varrho(\mathbb{S}(\mathbf{s}))}. \quad (36)$$

A difficulty arising in the re-sampling approach is that if the safe set $\mathbb{S}(\mathbf{s})$ is not trivial, evaluating (36) can only be done via sampling techniques. Sampling techniques are computationally efficient only if verifying the condition $\mathbf{a} \in \mathbb{S}(\mathbf{s})$ is inexpensive. This is unfortunately not the case in the NMPC context, where verifying $\mathbf{a} \in \mathbb{S}(\mathbf{s})$ requires solving an NLP, or at least a feasibility problem. Furthermore, evaluating the gradient of the measure $\nabla_\theta \mu_\varrho(\mathbb{S}(\mathbf{s}))$ via sampling is in general even more difficult.

B. Safe stochastic policy via softmax

We consider next a classic approach in RL to generate stochastic policies, based on the softmax approach, but adapted to the optimization-based policy approximation. Consider the following modification of (21), based on the primal interior-point method [8], using a logarithmic barrier:

$$\begin{aligned} \Phi_\tau^*(\mathbf{a}, \mathbf{s}, \theta) &= \\ \min_{\mathbf{u}} \quad &\Phi(\mathbf{x}, \mathbf{u}, \theta) - \tau \sum_i \log(\mathbf{h}_i(\mathbf{x}, \mathbf{u}, \theta)) \quad (37a) \\ \text{s.t.} \quad &\mathbf{f}(\mathbf{x}, \mathbf{u}, \mathbf{s}, \theta) = 0, \quad (37b) \\ &\mathbf{u}_0 = \mathbf{a}. \quad (37c) \end{aligned}$$

Infeasible inputs \mathbf{a} ought to be treated by assigning an infinite value to Φ_τ^* . A stochastic policy can then be defined as a softmax [18] over the cost of (37), i.e.:

$$\pi_\theta[\mathbf{a}|\mathbf{s}] \propto e^{-\Phi_\tau^*(\mathbf{a}, \mathbf{s}, \theta)}. \quad (38)$$

We then observe that the gradient of the score function can be obtained via NLP sensitivity techniques [15] and reads as

$$\nabla_\theta \log \pi_\theta[\mathbf{a}|\mathbf{s}] = -\nabla_\theta \Phi_\tau^*(\mathbf{a}, \mathbf{s}, \theta) = -\nabla_\theta \mathcal{L}, \quad (39)$$

where \mathcal{L} is the Lagrange function associated to (37), i.e.,

$$\mathcal{L}(\mathbf{x}, \mathbf{u}, \boldsymbol{\lambda}, \boldsymbol{\mu}, \theta) = \Phi - \tau \sum_i \mathbf{h}_i + \boldsymbol{\lambda}_0^\top (\mathbf{u}_0 - \mathbf{a}) + \boldsymbol{\lambda}^\top \mathbf{f}, \quad (40)$$

and $\boldsymbol{\lambda}$, $\boldsymbol{\lambda}_0$ are the multipliers associated to constraint (37b) and (37c), respectively.

Sampling the softmax policy (38) requires, in general, Importance Sampling techniques like the Metropolis-Hastings

Algorithm (MHA), allowing one to sample an arbitrary continuous distribution. The difficulty with such techniques is that they typically require a large number of evaluations of (37) for generating each sample of $\pi_\theta[\mathbf{a}|\mathbf{s}]$. Hence, while the simplicity of this approach is appealing, it presents the significant drawbacks that sampling policy (38) can be very expensive. This difficulty is arguably alleviated in the static case (22), where (37) simplifies to:

$$\Phi_\tau^*(\mathbf{a}, \mathbf{s}, \theta) = \Phi(\mathbf{s}, \mathbf{a}, \theta) - \tau \sum_i \log(\mathbf{h}_i(\mathbf{s}, \mathbf{a}, \theta)), \quad (41)$$

and the evaluation of (38) reduces to an evaluation of the cost and constraints in (41). We now turn to another option for building safe policies, which is more adequate for a deployment in the NMPC case.

C. Optimization-based safe stochastic policy

We will consider a stochastic policy that generates control inputs

$$\mathbf{a} \sim \pi_\theta[\mathbf{a}|\mathbf{s}] \quad (42)$$

computed from $\mathbf{a} = \mathbf{u}_0^d(\mathbf{s}, \theta, \mathbf{d})$ where \mathbf{u}_0^d is generated by the randomly disturbed NLP

$$\mathbf{u}^d(\mathbf{s}, \theta, \mathbf{d}) = \arg \min_{\mathbf{u}} \Phi^d(\mathbf{x}, \mathbf{u}, \theta, \mathbf{d}) \quad (43a)$$

$$\text{s.t.} \quad \mathbf{f}(\mathbf{x}, \mathbf{u}, \mathbf{s}, \theta) = 0, \quad (43b)$$

$$\mathbf{h}(\mathbf{x}, \mathbf{u}, \theta) \leq 0, \quad (43c)$$

for an arbitrary cost function $\Phi^d(\mathbf{u}, \mathbf{s}, \theta, \mathbf{d})$, and where the parameter $\mathbf{d} \in \mathbb{R}^{n_a}$ is drawn from an arbitrary probability distribution, of density $\varrho(\mathbf{d}, \Sigma)$, which can, e.g., be a simple Gaussian distribution. One can readily observe that any realization of the inputs

$$\mathbf{a} = \mathbf{u}_0^d(\mathbf{s}, \theta, \mathbf{d}) \quad (44)$$

stemming from (43) is in $\mathbb{S}(\mathbf{s})$ by construction. A simple choice for the cost function $\Phi^d(\mathbf{u}, \mathbf{s}, \theta, \mathbf{d})$ is via a gradient disturbance:

$$\Phi^d(\mathbf{u}, \mathbf{s}, \theta, \mathbf{d}) = \Phi(\mathbf{u}, \mathbf{s}, \theta) + \mathbf{d}^\top \mathbf{u}_0. \quad (45)$$

The choice of cost (45) entails that the random variable \mathbf{d} yields a gradient disturbance in the original problem (21), and introduces stochasticity in the inputs \mathbf{a} generated.

One can readily observe that generating a sample from (42) requires one to only generate a sample from the chosen density $\varrho(\mathbf{d}, \Sigma)$ and to solve the disturbed NMPC problem (43). It is therefore dramatically less expensive than the resampling and softmax approach of Sections IV-A and IV-B. We will show next that computing the gradient of the score function of (42) does not require any sampling, provided that the adequate algorithmic tools are adopted.

V. POLICY GRADIENT FOR OPTIMIZATION-BASED SAFE STOCHASTIC POLICY

We develop next the gradient of the score function associated to (42)-(43). Unfortunately, a technical difficulty must be first alleviated here. Indeed, evaluating the stochastic policy

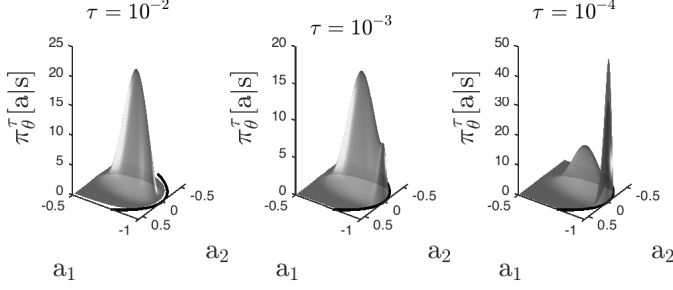


Fig. 1: Illustration of the stochastic policy resulting from (42)-(44) for different values of τ for a fixed \mathbf{s} , and \mathbf{u}_0^d restricted within a set $\mathbb{S}(\mathbf{s})$ depicted as the solid line. The resulting probability density $\pi_\theta^\tau[\mathbf{a}|\mathbf{s}]$ is constrained to remain within $\mathbb{S}(\mathbf{s})$. For very low values of τ , the density tends to a Dirac-like distribution on the border of the set, see right-side graph.

$\pi_\theta[\mathbf{a}|\mathbf{s}]$ resulting from (42)-(43) is in general very difficult, because it cannot be simply expressed as a function of the probability density $\varrho(\mathbf{d}, \Sigma)$. The mapping \mathbf{d} to \mathbf{u}_0^d generated by the NLP (43) is in general not bijective, as it acts as a (possibly nonlinear) projection operator of the distribution ϱ into the safe set $\mathbb{S}(\mathbf{s})$. A practical outcome of \mathbf{u}_0^d being non-bijective is that the resulting stochastic policy becomes Dirac-like on the boundary of the safe set $\mathbb{S}(\mathbf{s})$, see Fig. 1 for an illustration.

In order to alleviate this difficulty, similarly to the developments of Sec. IV-B, we will cast (43) in an interior-point context. For computational reasons, we will consider the primal-dual interior point formulation of (43) [8], which have the First-Order Necessary Conditions (FONC):

$$\mathbf{r}_\tau(\mathbf{z}, \boldsymbol{\theta}, \mathbf{d}) = \begin{bmatrix} \nabla_{\mathbf{w}} \Phi^d + \nabla_{\mathbf{w}} \mathbf{h} \boldsymbol{\mu} + \nabla_{\mathbf{w}} \mathbf{f} \boldsymbol{\lambda} \\ \mathbf{f} \\ \text{diag}(\boldsymbol{\mu}) \mathbf{h} + \tau \end{bmatrix} = 0 \quad (46)$$

for $\tau > 0$ and under the conditions $\mathbf{h} < 0$, $\boldsymbol{\mu} > 0$. Here we label $\mathbf{w} = \{\mathbf{u}, \mathbf{x}\}$ and $\mathbf{z} = \{\mathbf{w}, \boldsymbol{\lambda}, \boldsymbol{\mu}\}$ the primal-dual variables of (46). We will label $\mathbf{u}^\tau(\mathbf{s}, \boldsymbol{\theta}, \mathbf{d})$ the parametric primal solution of (46), and $\pi_\theta^\tau[\mathbf{a}|\mathbf{s}]$ the stochastic policy resulting from using $\mathbf{a} = \mathbf{u}_0^\tau(\mathbf{s}, \boldsymbol{\theta}, \mathbf{d})$. Under standard regularity assumptions [1] on (43), the algebraic conditions (46) admit a primal-dual solution that matches the solution of (43) with an accuracy at the order of the relaxation parameter τ . Moreover, the solution $\mathbf{u}^\tau(\mathbf{s}, \boldsymbol{\theta}, \mathbf{d})$ is guaranteed to satisfy the constraints of (43), hence it delivers safe policies. Additionally, (46) is smooth and the mapping \mathbf{d} to \mathbf{u}_0^d becomes bijective under some mild conditions. We therefore propose to use (46) as a smooth surrogate for (43). We will then use the sensitivities of (46) to compute the gradient of the score function of π_θ^τ .

Fig. 1 provides an illustration of the stochastic policy delivered by (46) for different values of τ , and how the stochastic policy adopts a Dirac-like shape on the border of the safety set when $\tau \rightarrow 0$.

In the following, we will use the notation \mathbf{g} for the first block of m inputs resulting from (46), i.e.:

$$\mathbf{g}(\mathbf{s}, \boldsymbol{\theta}, \mathbf{d}) = \mathbf{u}_0^\tau(\mathbf{s}, \boldsymbol{\theta}, \mathbf{d}) \approx \mathbf{u}_0^d(\mathbf{s}, \boldsymbol{\theta}, \mathbf{d}), \quad (47)$$

delivering \mathbf{a} from (46). The stochastic policy π_θ then results from the transformation of the probability density $\mathbf{d} \sim \varrho(\mathbf{d}, \Sigma)$ via \mathbf{g} , and can be evaluated using [7]

$$\pi_\theta[\mathbf{a}|\mathbf{s}] = \varrho(\mathbf{g}^{-1}, \Sigma) \det \left(\frac{\partial \mathbf{g}^{-1}}{\partial \mathbf{a}} \right) \bigg|_{\mathbf{a}, \boldsymbol{\theta}, \mathbf{s}}, \quad (48)$$

where function \mathbf{g}^{-1} is such that

$$\mathbf{d} = \mathbf{g}^{-1}(\mathbf{a}, \boldsymbol{\theta}, \mathbf{s}) \quad (49)$$

for any \mathbf{d} and associated \mathbf{a} delivered by (47). The (local) existence of \mathbf{g}^{-1} is guaranteed by the implicit function theorem if $\frac{\partial \mathbf{g}}{\partial \mathbf{d}}$ is full rank. We will use (48) to compute the gradient of the score function of π_θ .

For the sake of completeness, we provide hereafter a Lemma establishing the rank of $\frac{\partial \mathbf{g}}{\partial \mathbf{d}}$ for the gradient disturbance strategy (45).

Lemma 1: For the choice of cost function (45), and if (43) satisfies LICQ and SOSC, the Jacobian $\frac{\partial \mathbf{g}}{\partial \mathbf{d}}$ of function \mathbf{g} implicitly defined by (46)-(47) is full rank for any $\tau > 0$.

Proof: for the sake of simplicity, we will prove the result using the primal interior-point conditions corresponding to (46). The Lemma will then hold from the equivalence between the primal-dual and primal interior-point problem [15]. The primal interior-point conditions read as [15]:

$$\begin{bmatrix} \nabla_{\mathbf{w}} \Phi^d + \tau \nabla_{\mathbf{w}} \mathbf{h} \text{diag}(\mathbf{h})^{-1} + \nabla_{\mathbf{w}} \mathbf{f} \boldsymbol{\lambda} \\ \mathbf{f} \end{bmatrix} = 0. \quad (50)$$

The Implicit Function Theorem (IFT) then guarantees that:

$$\begin{bmatrix} H & \nabla_{\mathbf{w}} \mathbf{f} \\ \nabla_{\mathbf{w}} \mathbf{f}^\top & 0 \end{bmatrix} \begin{bmatrix} \frac{\partial \mathbf{w}}{\partial \mathbf{d}} \\ \frac{\partial \boldsymbol{\lambda}}{\partial \mathbf{d}} \end{bmatrix} = - \begin{bmatrix} \nabla_{\mathbf{w}} \Phi^d \\ 0 \end{bmatrix}, \quad (51)$$

where H is the Jacobian of the first row in (50). Defining \mathcal{N} the null space of $\nabla_{\mathbf{w}} \mathbf{f}^\top$, i.e., $\nabla_{\mathbf{w}} \mathbf{f}^\top \mathcal{N} = 0$, one can verify that using $\nabla_{\mathbf{u}_0^d} \Phi^d = I_{n_a \times n_a}$ from (45):

$$\frac{\partial \mathbf{w}}{\partial \mathbf{d}} = -\mathcal{N} (\mathcal{N}^\top H \mathcal{N})^{-1} \mathcal{N}^\top \nabla_{\mathbf{w}} \Phi^d \quad (52)$$

$$= -\mathcal{N} (\mathcal{N}^\top H \mathcal{N})^{-1} \mathcal{N}_0^\top, \quad (53)$$

where $\mathcal{N}_0 = [I_{n_a \times n_a} \ 0 \ \dots \ 0] \mathcal{N}$. The invertibility of $\mathcal{N}^\top H \mathcal{N}$ is guaranteed if (43) satisfies LICQ and SOSC. It follows that

$$\frac{\partial \mathbf{g}}{\partial \mathbf{d}} = -\mathcal{N}_0 (\mathcal{N}^\top H \mathcal{N})^{-1} \mathcal{N}_0^\top. \quad (54)$$

Since the dynamics \mathbf{f} cannot restrict the input \mathbf{u} in (43), \mathcal{N} spans the full space of \mathbf{u} , and therefore \mathcal{N} must span the full input space for \mathbf{u}_0 , such that \mathcal{N}_0 is full rank. As a result, (54) is full rank. ■

One can observe that Lemma 1 is also trivially valid in the static case. We ought to caveat Lemma 1 by observing that while matrix $\frac{\partial \mathbf{g}}{\partial \mathbf{d}}$ is full rank for any $\tau > 0$, it can nonetheless tend to a rank-deficient matrix for $\tau \rightarrow 0$. This issue will be discussed in Proposition 2 and in the following remarks.

The following Lemma provides the sensitivity of function (49), which will be required to compute the stochastic policy gradient.

Lemma 2: If (43) satisfies SOSC and LICQ then the following equalities hold:

$$\frac{\partial \mathbf{g}^{-1}}{\partial \boldsymbol{\theta}} = - \left(\frac{\partial \mathbf{g}}{\partial \mathbf{d}} \right)^{-1} \frac{\partial \mathbf{g}}{\partial \boldsymbol{\theta}}, \quad (55a)$$

$$\frac{\partial \mathbf{g}^{-1}}{\partial \mathbf{a}} = \left(\frac{\partial \mathbf{g}}{\partial \mathbf{d}} \right)^{-1}, \quad (55b)$$

for any $\mathbf{a}, \boldsymbol{\theta}, \mathbf{s}$ and $\mathbf{d} = \mathbf{g}^{-1}(\mathbf{a}, \boldsymbol{\theta}, \mathbf{s})$.

Proof: We observe that

$$\mathbf{g}(\mathbf{s}, \boldsymbol{\theta}, \mathbf{g}^{-1}(\mathbf{a}, \boldsymbol{\theta}, \mathbf{s})) = \mathbf{a}, \quad \forall \mathbf{a}, \boldsymbol{\theta}, \mathbf{s}. \quad (56)$$

It follows that

$$\frac{\mathrm{d}}{\mathrm{d}\boldsymbol{\theta}} \mathbf{g}(\mathbf{s}, \boldsymbol{\theta}, \mathbf{g}^{-1}(\mathbf{a}, \boldsymbol{\theta}, \mathbf{s})) = \frac{\partial \mathbf{g}}{\partial \boldsymbol{\theta}} + \frac{\partial \mathbf{g}}{\partial \mathbf{d}} \frac{\partial \mathbf{g}^{-1}}{\partial \boldsymbol{\theta}} = 0, \quad (57)$$

which establishes (55a). Moreover, we observe that

$$\frac{\mathrm{d}}{\mathrm{d}\mathbf{a}} \mathbf{g}(\mathbf{s}, \boldsymbol{\theta}, \mathbf{g}^{-1}(\mathbf{a}, \boldsymbol{\theta}, \mathbf{s})) = \frac{\partial \mathbf{g}}{\partial \mathbf{d}} \frac{\partial \mathbf{g}^{-1}}{\partial \mathbf{a}} = \mathbf{I}, \quad (58)$$

which establishes (55b). ■

A. Gradient of the score function

We can then use (48) to develop expressions for computing the gradient of the policy score function $\nabla_{\boldsymbol{\theta}} \log \pi_{\boldsymbol{\theta}}$. This is detailed in the following Proposition.

Proposition 1: The gradient of the score function for a given realization of \mathbf{a} obtained from a realization of \mathbf{d} via solving (43) reads as:

$$\nabla_{\boldsymbol{\theta}} \log \pi_{\boldsymbol{\theta}}[\mathbf{a} | \mathbf{s}] = \mathbf{m} - \left(\varrho^{-1} \frac{\partial \varrho}{\partial \mathbf{d}} \left(\frac{\partial \mathbf{g}}{\partial \mathbf{d}} \right)^{-1} \frac{\partial \mathbf{g}}{\partial \boldsymbol{\theta}} \right)^{\top}, \quad (59)$$

evaluated at $\mathbf{s}, \boldsymbol{\theta}, \mathbf{d}$, and where

$$\mathbf{m}_i = \text{Tr} \left(\frac{\partial \mathbf{g}}{\partial \mathbf{d}} \frac{\mathrm{d}}{\mathrm{d}\boldsymbol{\theta}_i} \frac{\partial \mathbf{g}^{-1}}{\partial \mathbf{a}} \right) \Big|_{\mathbf{s}, \boldsymbol{\theta}, \mathbf{d}, \mathbf{a}}. \quad (60)$$

Computational techniques to evaluate (59)-(60) are provided in Section V-B.

Proof: Using (48), the score function of $\pi_{\boldsymbol{\theta}}[\mathbf{a} | \mathbf{s}]$ is given by:

$$\log \pi_{\boldsymbol{\theta}}[\mathbf{a} | \mathbf{s}] = \log \varrho(\mathbf{g}^{-1}, \Sigma) - \log \det \left(\frac{\partial \mathbf{g}^{-1}}{\partial \mathbf{a}} \right). \quad (61)$$

Using (55a) we observe that:

$$\begin{aligned} \nabla_{\boldsymbol{\theta}} \log \varrho(\mathbf{g}^{-1}, \Sigma) &= \left(\varrho^{-1} \frac{\partial \varrho}{\partial \mathbf{d}} \frac{\partial \mathbf{g}^{-1}}{\partial \boldsymbol{\theta}} \right)^{\top} \Big|_{\mathbf{s}, \boldsymbol{\theta}, \mathbf{d}} \\ &= - \left(\varrho^{-1} \frac{\partial \varrho}{\partial \mathbf{d}} \left(\frac{\partial \mathbf{g}}{\partial \mathbf{d}} \right)^{-1} \frac{\partial \mathbf{g}}{\partial \boldsymbol{\theta}} \right)^{\top} \Big|_{\mathbf{s}, \boldsymbol{\theta}, \mathbf{d}}, \end{aligned} \quad (62)$$

hence providing the second term in (59). From calculus and using (55b), we get:

$$\begin{aligned} \frac{\mathrm{d}}{\mathrm{d}\boldsymbol{\theta}_i} \log \det \left(\frac{\partial \mathbf{g}^{-1}}{\partial \mathbf{a}} \right) &= \text{Tr} \left(\left(\frac{\partial \mathbf{g}^{-1}}{\partial \mathbf{a}} \right)^{-1} \frac{\mathrm{d}}{\mathrm{d}\boldsymbol{\theta}_i} \frac{\partial \mathbf{g}^{-1}}{\partial \mathbf{a}} \right) \\ &= \text{Tr} \left(\frac{\partial \mathbf{g}}{\partial \mathbf{d}} \frac{\mathrm{d}}{\mathrm{d}\boldsymbol{\theta}_i} \frac{\partial \mathbf{g}^{-1}}{\partial \mathbf{a}} \right) = \mathbf{m}_i, \end{aligned} \quad (63)$$

hence providing (60) component-wise. ■

We now turn to detailing how the sensitivities of functions \mathbf{g} and \mathbf{g}^{-1} can be computed at limited computational cost.

B. Sensitivity computation

We provide hereafter some expressions allowing one to evaluate the terms in (59)-(60). First, it is useful to provide the sensitivities of function $\mathbf{g} = \mathbf{z}_0$, where \mathbf{z}_0 is the first m elements of \mathbf{z} , solution of (46). If LICQ and SOSC hold [15] for the NLP (43), one can verify that the Implicit Function Theorem (IFT) guarantees that:

$$\frac{\partial \mathbf{r}_{\tau}}{\partial \mathbf{z}} \frac{\partial \mathbf{z}}{\partial \mathbf{d}} + \frac{\partial \mathbf{r}_{\tau}}{\partial \mathbf{d}} = 0, \quad \frac{\partial \mathbf{r}_{\tau}}{\partial \mathbf{z}} \frac{\partial \mathbf{z}}{\partial \boldsymbol{\theta}} + \frac{\partial \mathbf{r}_{\tau}}{\partial \boldsymbol{\theta}} = 0 \quad (64)$$

and therefore $\frac{\partial \mathbf{g}}{\partial \mathbf{d}}$ and $\frac{\partial \mathbf{g}}{\partial \boldsymbol{\theta}}$, required in the second term of (59), can be extracted from the m first rows of $\frac{\partial \mathbf{z}}{\partial \mathbf{d}}$ and $\frac{\partial \mathbf{z}}{\partial \boldsymbol{\theta}}$ obtained by solving the linear system (64).

Obtaining the second-order term $\frac{\partial^2 \mathbf{g}^{-1}}{\partial \boldsymbol{\theta}_i \partial \mathbf{a}}$ in (63) can be fairly involved. In order to simplify its computation, we propose to use the following approach. Let us define:

$$\tilde{\mathbf{z}} = \{\mathbf{d}, \mathbf{u}_1, \dots, \mathbf{u}_{N-1}, \mathbf{x}, \boldsymbol{\lambda}, \boldsymbol{\mu}\}, \quad (65)$$

given implicitly by (46) as a function of $\mathbf{s}, \boldsymbol{\theta}, \mathbf{a}$ given. One can then construe $\tilde{\mathbf{z}}$ and therefore \mathbf{d} as an implicit function of $\mathbf{s}, \boldsymbol{\theta}, \mathbf{u}_0$, with $\mathbf{u}_0 = \mathbf{a}$, defined by (46). It follows that function $\mathbf{g}^{-1} = \tilde{\mathbf{z}}_0$, i.e., function \mathbf{g}^{-1} is given by the m first entries of $\tilde{\mathbf{z}}$, implicitly defined by (46). The IFT then naturally applies and delivers:

$$\frac{\partial \mathbf{r}_{\tau}}{\partial \tilde{\mathbf{z}}} \frac{\partial \tilde{\mathbf{z}}}{\partial \mathbf{a}} + \frac{\partial \mathbf{r}_{\tau}}{\partial \mathbf{u}_0} = 0, \quad \frac{\partial \mathbf{r}_{\tau}}{\partial \tilde{\mathbf{z}}} \frac{\partial \tilde{\mathbf{z}}}{\partial \boldsymbol{\theta}} + \frac{\partial \mathbf{r}_{\tau}}{\partial \boldsymbol{\theta}} = 0 \quad (66)$$

such that $\frac{\partial \mathbf{g}^{-1}}{\partial \mathbf{a}}, \frac{\partial \mathbf{g}^{-1}}{\partial \boldsymbol{\theta}}$ can be extracted from the m first rows of $\frac{\partial \tilde{\mathbf{z}}}{\partial \mathbf{a}}, \frac{\partial \tilde{\mathbf{z}}}{\partial \boldsymbol{\theta}}$, obtained by solving the linear system (66). The second-order term $\frac{\partial^2 \mathbf{g}^{-1}}{\partial \boldsymbol{\theta}_i \partial \mathbf{a}}$ in (63) can be obtained from solving the second-order sensitivity equation of the NLP:

$$\begin{aligned} \frac{\partial \mathbf{r}_{\tau}}{\partial \tilde{\mathbf{z}}} \frac{\partial^2 \tilde{\mathbf{z}}}{\partial \boldsymbol{\theta}_i \partial \mathbf{a}} + \left(\frac{\partial^2 \mathbf{r}_{\tau}}{\partial \boldsymbol{\theta}_i \partial \tilde{\mathbf{z}}} + \sum_j \frac{\partial^2 \mathbf{r}_{\tau}}{\partial \tilde{\mathbf{z}} \partial \mathbf{z}_j} \frac{\partial \tilde{\mathbf{z}}_j}{\partial \boldsymbol{\theta}_i} \right) \frac{\partial \tilde{\mathbf{z}}}{\partial \mathbf{a}} + \frac{\partial^2 \mathbf{r}_{\tau}}{\partial \boldsymbol{\theta}_i \partial \mathbf{a}} \\ + \sum_j \frac{\partial^2 \mathbf{r}_{\tau}}{\partial \mathbf{a} \partial \tilde{\mathbf{z}}_j} \frac{\partial \tilde{\mathbf{z}}_j}{\partial \boldsymbol{\theta}_i} = 0. \end{aligned} \quad (67)$$

One can solve the linear system (67) for $\frac{\partial^2 \tilde{\mathbf{z}}}{\partial \boldsymbol{\theta}_i \partial \mathbf{a}}$, and therefore obtain $\frac{\partial^2 \mathbf{g}^{-1}}{\partial \boldsymbol{\theta}_i \partial \mathbf{a}}$.

We ought to underline here that the linear systems (64), (66) and (67) are large but very sparse if coming from an NMPC scheme. Their sparsity ought to be exploited for computational efficiency both when forming and solving the systems. Unfortunately, the computational complexity of evaluating the linear system (67) grows with the number of parameters $\boldsymbol{\theta}$, which is unfavorable for rich parametrizations of the policy.

C. Limit case of the gradient of the score function

One ought to observe that matrix $\frac{\partial \mathbf{g}}{\partial \mathbf{d}}$ becomes asymptotically ($\tau \rightarrow 0$) rank deficient if some constraints are active at the first stage $k = 0$, hence restricting \mathbf{a} on some manifold of \mathbb{R}^{n_a} . As a result, it is not obvious that the terms involved in (59) and (63) are asymptotically well defined for $\tau \rightarrow 0$. The following proposition alleviates this concern in some cases. The other cases are discussed after the Proposition.

Proposition 2: For the choice of cost function (45), and if the MPC model dynamics and constraints are not depending on the parameters, i.e., $\nabla_{\theta} \mathbf{h} = 0$, $\nabla_{\theta} \mathbf{f} = 0$, and if $\frac{\partial \nabla_{\mathbf{w}}^2 \Phi^d}{\partial \theta} = 0$ then the expressions

$$\left(\frac{\partial \mathbf{g}}{\partial \mathbf{d}} \right)^{-1} \frac{\partial \mathbf{g}}{\partial \theta}, \quad \left(\frac{\partial \mathbf{g}}{\partial \mathbf{d}} \right)^{-1} \nabla_{\theta_i} \frac{\partial \mathbf{g}}{\partial \theta}, \quad (68)$$

are well defined for $\tau \rightarrow 0$ if Problem (43) fulfils LICQ and SOSC.

Proof: We will proceed with proving that the expressions (68) are well defined in the sense of the pseudo-inverse in an active-set setting deployed on (43). The asymptotic result (68) will then hold from the convergence of the Interior-Point solution to the active-set one. Consider \mathbb{A} the (strictly) active set of (43), i.e., the set of indices i such that $\mathbf{h}_i = 0$, $\mu_i > 0$ at the solution. We observe that

$$\begin{bmatrix} H & \nabla_{\mathbf{w}} \mathbf{q} \\ \nabla_{\mathbf{w}} \mathbf{q}^\top & 0 \end{bmatrix} \begin{bmatrix} \frac{\partial \mathbf{w}}{\partial \mathbf{d}} \\ \frac{\partial \nu}{\partial \mathbf{d}} \end{bmatrix} = - \begin{bmatrix} \nabla_{\mathbf{w}} \Phi^d \\ 0 \end{bmatrix}, \quad (69)$$

where H is the Hessian of the Lagrange function associated to (43) and

$$\mathbf{q} = \begin{bmatrix} \mathbf{f} \\ \mathbf{h}_{\mathbb{A}} \end{bmatrix}, \quad \nu = \begin{bmatrix} \lambda \\ \mu_{\mathbb{A}} \end{bmatrix}. \quad (70)$$

Defining $\mathcal{N}_{\mathbb{A}}$ the null space of $\nabla_{\mathbf{w}} \mathbf{q}^\top$, i.e. $\nabla_{\mathbf{w}} \mathbf{q}^\top \mathcal{N}_{\mathbb{A}} = 0$, and following the same line as in Lemma 1, we observe that:

$$\frac{\partial \mathbf{g}}{\partial \mathbf{d}} = -\mathcal{N}_{\mathbb{A}_0} (\mathcal{N}_{\mathbb{A}}^\top H \mathcal{N}_{\mathbb{A}})^{-1} \mathcal{N}_{\mathbb{A}_0}^\top, \quad (71)$$

where $\mathcal{N}_{\mathbb{A}_0} = \begin{bmatrix} I_{m \times m} & 0 & \dots & 0 \end{bmatrix} \mathcal{N}_{\mathbb{A}}$. Using a similar reasoning, since $\frac{\partial \nabla_{\mathbf{w}} \mathbf{q}}{\partial \theta} = 0$ and $\frac{\partial H}{\partial \theta} = 0$, we observe that:

$$\partial_{\theta}^k \mathbf{g} = -\mathcal{N}_{\mathbb{A}_0} (\mathcal{N}_{\mathbb{A}}^\top H \mathcal{N}_{\mathbb{A}})^{-1} \mathcal{N}_{\mathbb{A}}^\top \partial_{\theta}^k \nabla_{\mathbf{w}} \Phi^d, \quad (72)$$

where ∂_{θ}^k are multi-indexed differential operators with respect to θ , using any multi index k . This entails that $\partial_{\theta}^k \mathbf{g}$ can be expressed as $\partial_{\theta}^k \mathbf{g} = \mathcal{N}_{\mathbb{A}_0} Q$ for some matrix Q . Consider then the linear system in the unknown matrix X :

$$\frac{\partial \mathbf{g}}{\partial \mathbf{d}} X + \partial_{\theta}^k \mathbf{g} = 0. \quad (73)$$

Since $\mathcal{N}_{\mathbb{A}}^\top H \mathcal{N}_{\mathbb{A}}$ is full rank, $\mathcal{N}_{\mathbb{A}_0} Q$ is in the span of matrix $\mathcal{N}_{\mathbb{A}_0} (\mathcal{N}_{\mathbb{A}}^\top H \mathcal{N}_{\mathbb{A}})^{-1} \mathcal{N}_{\mathbb{A}_0}^\top$. It follows that (73) is consistent, such that it can be solved for X using, e.g., a pseudo-inverse. As a result, by continuity of the solution manifold defined by (46), the expressions (68) have a well-defined limit for $\tau \rightarrow 0$, given by the solution of the linear system (73). ■

It is important to note here that Proposition 2 relies on the safety constraints \mathbf{h} being independent of the parameters θ . This requirement is not an artificial effect of the approach, but rather a fundamental limitation of deploying the stochastic policy gradient approach on safety sets. Indeed, one can observe that the probability density $\pi_{\theta}[\mathbf{a} | \mathbf{s}]$ can be discontinuous at the border $\partial \mathbb{S}(\mathbf{s})$ of the set $\mathbb{S}(\mathbf{s})$ defined by \mathbf{h} , as the probability density is (possibly) non-zero at $\partial \mathbb{S}(\mathbf{s})$ and zero outside. As a result, the gradient $\nabla_{\theta} \log \pi_{\theta}[\mathbf{a} | \mathbf{s}]$ can be ill-defined for $\mathbf{a} \in \partial \mathbb{S}(\mathbf{s})$ if the changes in the parameters θ can move the set border $\partial \mathbb{S}(\mathbf{s})$. The Interior-Point approach proposed in Section IV-C alleviates

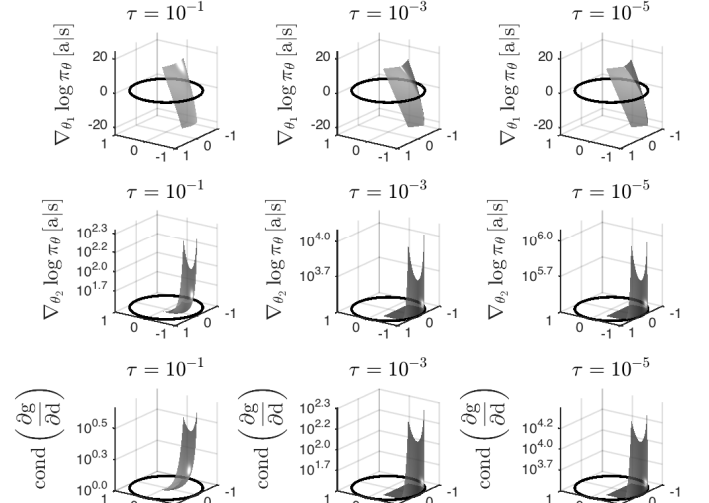


Fig. 2: Illustration of the gradient of the stochastic policy resulting from (42)-(44) for different values of τ , \mathbf{s} fixed, and \mathbf{u}_0^d restricted within a set $\mathbb{S}(\mathbf{s})$ depicted as the solid circle. The first row of graphs depict the gradient with respect to parameter θ_1 for which $\nabla_{\theta_1} \mathbf{h}$, $\nabla_{\theta_1} \mathbf{f} = 0$, while the second row depicts the gradient with respect to parameter θ_2 for which $\nabla_{\theta_2} \mathbf{h} \neq 0$. The last row depicts the conditioning of matrix $\frac{\partial \mathbf{g}}{\partial \mathbf{d}}$. As predicted by Proposition 2 for $\tau \rightarrow 0$, $\frac{\partial \mathbf{g}}{\partial \mathbf{d}}$ tends to a rank-deficient matrix for $\mathbf{a} = \mathbf{u}_0^d \rightarrow \partial \mathbb{S}(\mathbf{s})$, and the gradient $\nabla_{\theta_2} \log \pi_{\theta}$ degenerates while $\nabla_{\theta_1} \log \pi_{\theta}$ does not.

this problem, at the expense of keeping τ finite rather than using $\tau \rightarrow 0$. The problem is avoided by smoothing the transition from a non-zero density in $\mathbb{S}(\mathbf{s})$ to a zero density outside. These observations are illustrated in Figures 1-2.

VI. SAFE RL STEPS

The methodology described so far allows one to deploy a safe policy and safe exploration using a robust NMPC scheme, in order to compute the deterministic policy gradient, and determine directions in the parameter space θ that improve the closed-loop performance of the resulting control policy. However, taking a step in θ can arguably jeopardise the safety of the policy, e.g., by modifying the constraints, or the models underlying the robust NMPC scheme. The problem of modifying the NMPC parameters while maintaining safety is arguably a complex one, and beyond the scope of this paper. However, in the robust linear MPC context detailed in Section III-B, there is a simple approach to handle this problem, which we detail here. We observe that a classic gradient step of step-size $\alpha > 0$ reads as:

$$\theta = \theta_- - \alpha \nabla_{\theta} J \quad (74)$$

where θ_- is the previous vector of parameters. One can trivially observe that the gradient step can be construed as

the solution of the optimization problem:

$$\min_{\boldsymbol{\theta}} \frac{1}{2} \|\boldsymbol{\theta} - \boldsymbol{\theta}_-\|^2 + \alpha \nabla_{\boldsymbol{\theta}} J^\top (\boldsymbol{\theta} - \boldsymbol{\theta}_-). \quad (75)$$

Imposing the data-driven safe-design constraints (31) on the gradient step generating the new parameters can then simply be cast as the following constrained optimization problem:

$$\min_{\boldsymbol{\theta}, \boldsymbol{\vartheta}} \frac{1}{2} \|\boldsymbol{\theta} - \boldsymbol{\theta}_-\|^2 + \alpha \nabla_{\boldsymbol{\theta}} J^\top (\boldsymbol{\theta} - \boldsymbol{\theta}_-) \quad (76a)$$

$$\text{s.t. } \mathbf{s}_{k+1} - \mathbf{F}_0(\mathbf{s}_k, \mathbf{a}_k, \boldsymbol{\theta}) - \sum_{i=1}^V \sum_{k=0}^{N_D} \boldsymbol{\vartheta}_{i,k} \mathbf{W}^i = 0, \quad (76b)$$

$$\sum_{i=1}^V \boldsymbol{\vartheta}_{i,k} = 1, \quad \forall k = 0, \dots, N_D, \quad (76c)$$

$$\boldsymbol{\vartheta}_{i,k} \geq 0 \quad \forall k = 0, \dots, N_D, \quad i = 1, \dots, V, \quad (76d)$$

where (76b)-(76d) are the algebraic conditions testing (31). We observe that unfortunately the complexity of (76) grows with the amount of data N_D in use. In practice, the data set \mathcal{D} should arguably be limited to incorporate relevant state transitions. A data compression technique has been proposed in [21] to alleviate this issue in the case the nominal model \mathbf{F}_0 is fixed. Future work will improve on this baseline.

VII. IMPLEMENTATION & ILLUSTRATIVE EXAMPLE

In this section, we provide some details on how the principle presented in this paper can be implemented, and provide an illustrative example of this implementation. At each time instant k , for a given state \mathbf{s}_k , a sample is drawn from the stochastic policy $\pi_{\boldsymbol{\theta}}$, computed according to (46) with $\mathbf{d} \sim \varrho(\cdot, \Sigma)$. The gradient of the score function is then computed using (59). The data are collected to compute (12)-(13) either on-the-fly or in a batch fashion. The policy gradient estimation (12) is then used to compute the safe parameter update according to (76).

A. RL approach

In this example, the policy gradient was evaluated using batch Least-Squares Temporal-Difference (LSTD) techniques, whereby for each evaluation, the closed-loop system is run S times for N_t time steps, hence generating S trajectory samples of duration N_t . The value function estimations is constructed using:

$$\sum_{k=0}^{N_t} \sum_{i=1}^S \delta^V(\mathbf{s}_{k,i}, \mathbf{a}_{k,i}, \mathbf{s}_{k+1,i}) \nabla_{\mathbf{v}} \hat{V}_{\pi_{\boldsymbol{\theta}}}^{\mathbf{v}}(\mathbf{s}_{k,i}) = 0, \quad (77a)$$

$$\delta^V := L(\mathbf{s}_{k,i}, \mathbf{a}_{k,i}) + \gamma \hat{V}_{\pi_{\boldsymbol{\theta}}}^{\mathbf{v}}(\mathbf{s}_{k+1,i}) - \hat{V}_{\pi_{\boldsymbol{\theta}}}^{\mathbf{v}}(\mathbf{s}_{k,i}), \quad (77b)$$

using a linear value function approximation

$$\hat{V}^{\mathbf{v}}(\mathbf{s}) = \boldsymbol{\varrho}(\mathbf{s})^\top \mathbf{v}. \quad (78)$$

In this example, (78) uses a simple quadratic function in $\boldsymbol{\varrho}(\mathbf{s})$ to parametrize $\hat{V}^{\mathbf{v}}$.

We observe that (77) is linear in the parameters \mathbf{v} , and therefore straightforward to solve. However, it can be ill-posed

on some data sets, and ought to be solve using, e.g., a Moore-Penrose pseudo-inverse. The policy gradient estimation is then obtained using (12):

$$\widehat{\nabla_{\boldsymbol{\theta}} J(\pi_{\boldsymbol{\theta}})} = \sum_{k=0}^{N_t} \sum_{i=1}^S \nabla_{\boldsymbol{\theta}} \log \pi_{\boldsymbol{\theta}}(\mathbf{s}_{k,i}) \delta^V. \quad (79)$$

B. Robust linear MPC scheme

While the proposed theory is not limited to linear problems, for the sake of clarity, we propose to use a fairly simple robust linear MPC example using multiple models and process noise. We will consider the policy as delivered by the following robust MPC scheme based on multiple models and a linear feedback policy:

$$\min_{\mathbf{u}, \mathbf{x}} \sum_{j=0}^{N_M} \left(\|\mathbf{x}_{j,N} - \bar{\mathbf{x}}\|^2 + \sum_{k=0}^{N-1} \left\| \begin{bmatrix} \mathbf{x}_{j,k} - \bar{\mathbf{x}} \\ \mathbf{u}_{j,k} - \bar{\mathbf{u}} \end{bmatrix} \right\|^2 \right) \quad (80a)$$

$$\text{s.t. } \mathbf{x}_{j,k+1} = A_0 \mathbf{x}_{j,k} + B_0 \mathbf{u}_{j,k} + \mathbf{b}_0 + \mathbf{W}^j, \quad (80b)$$

$$\|\mathbf{x}_{j,k}\|^2 \leq 1, \quad \forall j = 0, \dots, N_M, k = 1, \dots, N, \quad (80c)$$

$$\mathbf{x}_{j,0} = \mathbf{s}, \quad \forall j = 1, \dots, N_M, \quad (80d)$$

$$\mathbf{u}_{j,0} = \mathbf{u}_{k,0}, \quad \forall k, j = 0, \dots, N_M, \quad (80e)$$

$$\mathbf{u}_{j,k} = \mathbf{u}_{0,k} - K(\mathbf{x}_{j,k} - \mathbf{x}_{0,k}), \quad j = 1, \dots, N_M, \quad (80f)$$

where A_0, B_0, \mathbf{b}_0 yield the MPC nominal model corresponding to \mathbf{F}_0 , with $\mathbf{W}^0 = 0$, and $\mathbf{W}^{1,\dots,M}$ capture the vertices of the dispersion set outer approximation. Hence model $j = 0$ serves as nominal model and models $j = 1, \dots, N_M$ capture the state dispersion over time. The linear feedback matrix K is possibly part of the MPC parameters $\boldsymbol{\theta}$, and is a (rudimentary) structure providing a feedback π^s as described in Section II-B. In practice, (80) is equivalent to a tube-based MPC.

C. Simulation setup & results

The simulations proposed here use the same setup as the companion paper [11] treating the stochastic policy gradient case, so as to make comparisons straightforward. The experimental parameters are summarized in Table I and:

$$\mathbf{x}_{k+1} = A_{\text{real}} \mathbf{x}_k + B_{\text{real}} \mathbf{u}_k + \mathbf{n}, \quad (81)$$

where the process noise \mathbf{n} is selected Normal centred, and clipped to a ball. The real system was selected as:

$$A_{\text{real}} = \kappa \begin{bmatrix} \cos \beta & \sin \beta \\ \sin \beta & \cos \beta \end{bmatrix}, B_{\text{real}} = \begin{bmatrix} 1.1 & 0 \\ 0 & 0.9 \end{bmatrix}. \quad (82)$$

The real process noise \mathbf{n} is chosen normal centred of covariance $\frac{1}{3}10^{-2}I$, and restricted to a ball of radius $\frac{1}{2}10^{-2}$. The initial nominal MPC model is chosen as:

$$A_0 = \begin{bmatrix} \cos \hat{\beta} & \sin \hat{\beta} \\ \sin \hat{\beta} & \cos \hat{\beta} \end{bmatrix}, B_0 = \begin{bmatrix} 1 & 0 \\ 0 & 1 \end{bmatrix}, \mathbf{b}_0 = \begin{bmatrix} 0 \\ 0 \end{bmatrix}. \quad (83)$$

and $N_M = 4$ with:

$$\mathbf{W}^1 = \frac{1}{10} \begin{bmatrix} -1 \\ -1 \end{bmatrix}, \quad \mathbf{W}^2 = \frac{1}{10} \begin{bmatrix} +1 \\ -1 \end{bmatrix} \quad (84a)$$

$$\mathbf{W}^3 = \frac{1}{10} \begin{bmatrix} +1 \\ +1 \end{bmatrix}, \quad \mathbf{W}^4 = \frac{1}{10} \begin{bmatrix} -1 \\ +1 \end{bmatrix}. \quad (84b)$$

TABLE I: Simulation parameters

Parameter	Value	Description
γ	0.99	Discount factor
Σ	I	Exploration shape
σ	10^{-3}	Exploration covariance
τ	10^{-2}	Relaxation parameter
β	22°	Real system parameter
$\hat{\beta}$	20°	Model parameter
N_t	20	Sample length
S	30	Number of sample per batch
N	10	MPC prediction horizon

The baseline stage cost is selected as:

$$L = \frac{1}{20} \|\mathbf{x} - \mathbf{x}_{\text{ref}}\|^2 + \frac{1}{2} \|\mathbf{u} - \mathbf{u}_{\text{ref}}\|^2 \quad (85)$$

and serves as the baseline performance criterion to evaluate the closed-loop performance of the MPC scheme.

We considered two cases, using deterministic initial conditions $\mathbf{s}_0 = [\cos 60^\circ \quad \sin 60^\circ]^\top$. Both cases consider the parameters $\boldsymbol{\theta} = \{\bar{\mathbf{x}}, \bar{\mathbf{u}}, A_0, B_0, \mathbf{b}_0, K, \mathbf{W}\}$. The first case considers a stable real system with $\kappa = 0.95$, the second case considers an unstable real system with $\kappa = 1.05$. In both cases, the target reference $\bar{\mathbf{x}}$ was provided, together with the input reference $\bar{\mathbf{u}}$ delivering a steady-state for the nominal MPC model. Table I reports the algorithmic parameters. Case 1 used a step size $\alpha = 0.05$, the second case used a step size $\alpha = 0.01$. The results for the first case are reported in Figures 3-7. One can observe in Fig. 3 that the closed-loop performance is improving over the RL steps. Figure 4 shows that the improvement takes place via driving the closed-loop trajectories of the real system closer to the reference, without jeopardising the system safety. Figure 5 shows how the RL algorithm uses the MPC nominal model to improve the closed-loop performance. One can readily see from Figure 5 that RL is not simply performing system identification, as the nominal MPC model developed by the RL algorithm does not tend to the real system dynamics. Figure 6 shows how the RL algorithm reshapes the dispersion set. The upper-left corner of the set is the most critical in terms of performance, as it activates the state constraint $\|\mathbf{x}\|^2 \leq 1$, and is moved inward to gain performance. The constrained RL step (76) ensures that the RL algorithm cannot jeopardize the system safety. In Figure 7, one can see that the RL algorithm does not use much the degrees of freedom provided by adapting the MPC feedback matrix K .

The results for case 2 are reported in Figures 8-12. Similar comments hold for case 2 as for case 1. The instability of the real system does not challenge the proposed algorithm, even though a smaller step size σ had to be used as the RL algorithm appears to more sensitive to noise.

VIII. CONCLUSION

This paper proposed a technique to deploy stochastic policy gradient methods where the stochastic policy is supported by a stochastically disturbed constrained parametric optimization problem. This approach allows one to restrict the support of

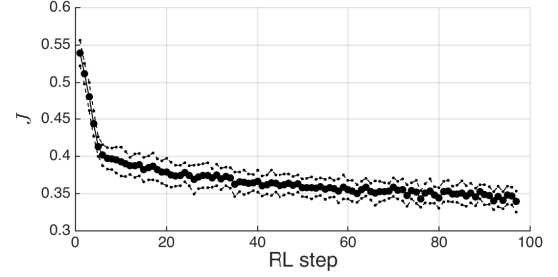


Fig. 3: Case 1. Evolution of the closed-loop performance J over the RL steps. The solid line represents the estimation of J based on the samples obtained in the batch. The dashed line represent the standard deviation due to the stochasticity of the system dynamics and policy disturbances.

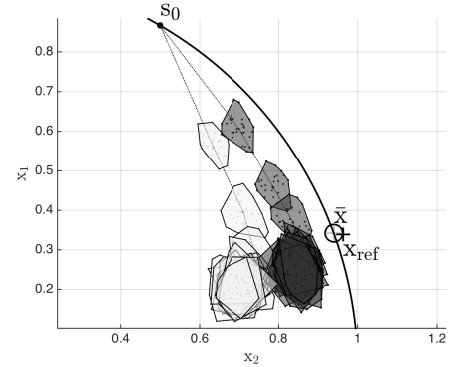


Fig. 4: Case 1. Closed-loop system trajectories. The initial conditions \mathbf{s}_0 are reported, as well as the target state reference \mathbf{x}_{ref} (circle), and the MPC reference $\bar{\mathbf{x}}$ at the first RL step and at the last one (grey and black + symbol respectively). The trajectories at the first and last RL steps are reported as the light and dark grey polytopes. The solid black curve represents the state constraint $\|\mathbf{x}\|^2 \leq 1$.

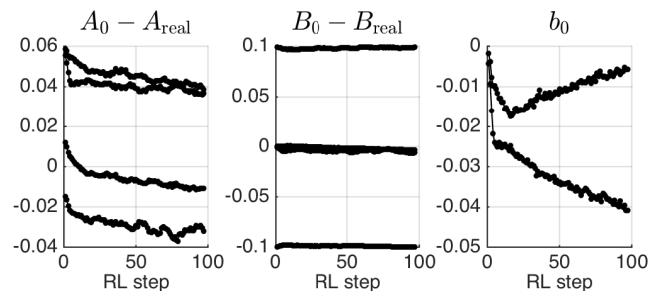


Fig. 5: Case 1. Evolution of the nominal MPC model over the RL steps. We report here the difference between the nominal model used in the MPC scheme and the real system.

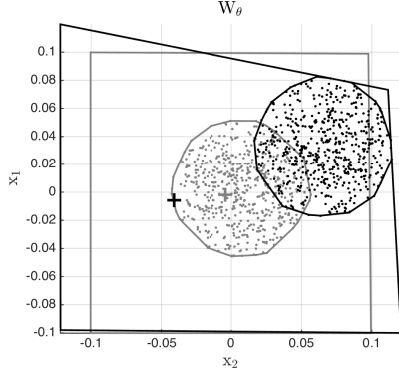


Fig. 6: Case 1. Evolution of the MPC model biases $\mathbf{W}^{1,\dots,M}$ over the RL steps. The light grey polytope depicts the biases at the first RL step, and the points show $\mathbf{s}_{k+1} - \mathbf{F}_0(\mathbf{s}_k, \mathbf{a}_k, \boldsymbol{\theta})$ for all the samples of the first batch of data. The cloud of point is inside the black thick quadrilateral thanks to the constrained RL step (76).

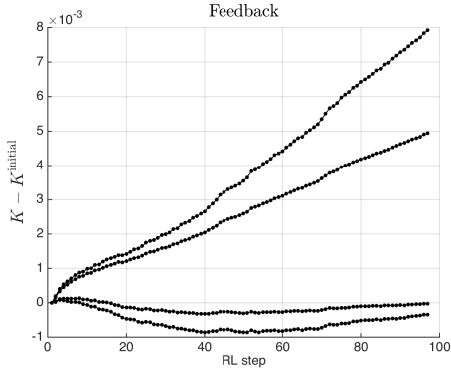


Fig. 7: Case 1. Evolution of the MPC feedback matrix K from its initial value. The feedback is only marginally adjusted by the RL algorithm. After 100 RL steps, the adaptation of the feedback gain K has not yet reached its steady-state value.

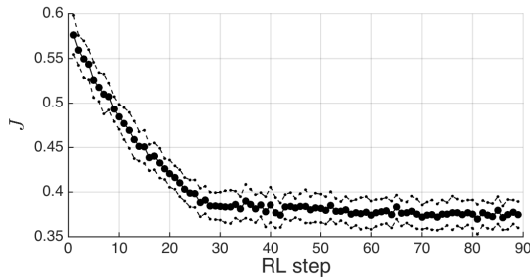


Fig. 8: Case 2, similar to Fig. 3.

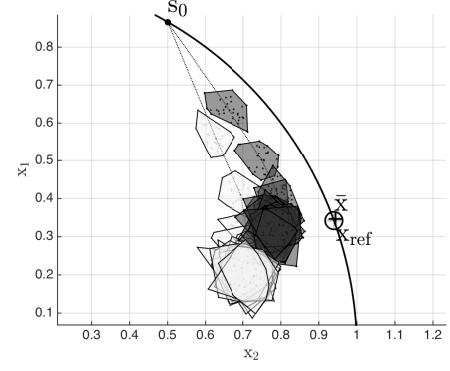


Fig. 9: Case 2, similar to Fig. 4

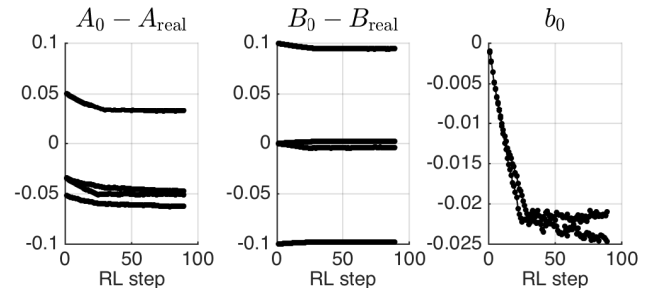


Fig. 10: Case 2, similar to 5.

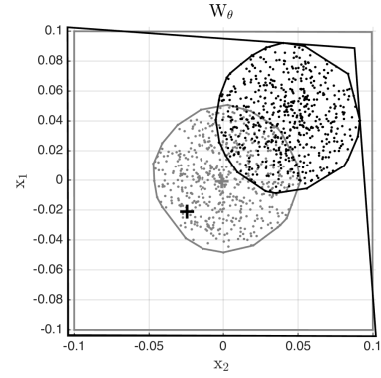


Fig. 11: Case 2, similar to Fig. 6.

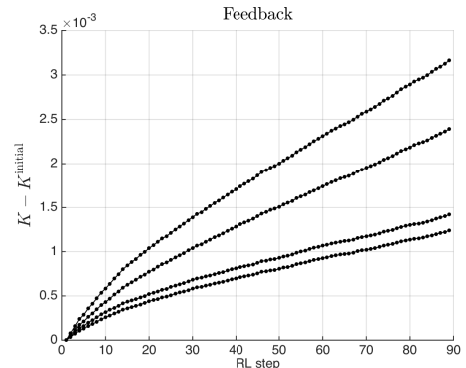


Fig. 12: Case 2, similar to Fig. 7.

the stochastic policy to a safe set described via constraints. In particular, robust Nonlinear Model Predictive Control, where safety requirements can be imposed explicitly, can be selected as a parametric optimization problem. Imposing restrictions on the support of the stochastic policy creates some technical challenges when computing the gradient of the policy score function required in the computation of the stochastic policy gradient. Computationally inexpensive methods are proposed here to tackle these challenges, using interior-point methods and techniques from parametric Nonlinear Programming. The specific case of robust linear Model Predictive Control, where the prediction model is linear, is further developed, and a methodology to impose safety requirements throughout the learning is proposed. The proposed techniques are illustrated in simple simulations, showing their behavior. This paper has a companion paper [11] investigating the deterministic policy gradient approach in the same context as in this paper. The stochastic policy gradient approach is theoretically simple and appealing, and requires less assumptions than its deterministic counterpart presented in [11]. It also requires solving a single NLP per time instant, as opposed to two in the deterministic case. However, the computational complexity of the stochastic approach presented here can be significantly higher than the deterministic policy approach of [11] when the number of parameters θ is larger than the input size n_a . This effect is a direct result of the computational complexity of evaluating the second-order sensitivities required to form the gradient of the stochastic policy score function, see (67).

REFERENCES AND NOTES

- [1] Pieter Abbeel, Adam Coates, Morgan Quigley, and Andrew Y. Ng. An application of reinforcement learning to aerobatic helicopter flight. In *Advances in Neural Information Processing Systems 19*, page 2007. MIT Press, 2007.
- [2] D. Bernardini and A. Bemporad. Scenario-based model predictive control of stochastic constrained linear systems. In *Proceedings of the 48th IEEE Conference on Decision and Control (CDC) held jointly with 2009 28th Chinese Control Conference*, pages 6333–6338, Dec 2009.
- [3] D. Bertsekas. *Dynamic Programming and Optimal Control*, volume 2. Athena Scientific, 3rd edition, 2007.
- [4] D.P. Bertsekas. *Dynamic Programming and Optimal Control*, volume 1 and 2. Athena Scientific, Belmont, MA, 1995.
- [5] D.P. Bertsekas and I.B. Rhodes. Recursive state estimation for a set-membership description of uncertainty. *IEEE Transactions on Automatic Control*, 16:117–128, 1971.
- [6] D.P. Bertsekas and S.E. Shreve. *Stochastic Optimal Control: The Discrete Time Case*. Athena Scientific, Belmont, MA, 1996.
- [7] D.P. Bertsekas and J.N. Tsitsiklis. *Optimum Experimental Designs*. Mass. : Athena Scientific, Belmont, 2002.
- [8] Lorenz T. Biegler. *Nonlinear Programming*. MOS-SIAM Series on Optimization. SIAM, 2010.
- [9] T. Ensslin. *Information Field Theory*. arXiv:1301.2556 [astro-ph.IM], 2013.
- [10] S. Gros and M. Zanon. Data-Driven Economic NMPC using Reinforcement Learning. *IEEE Transactions on Automatic Control*, 2018. (in press).
- [11] S. Gros and M. Zanon. Towards Safe Reinforcement Learning Using NMPC and Policy Gradients - Deterministic case (Part II). *IEEE Transactions on Automatic Control*, 2019. (submitted).
- [12] J. Fernandez J. Garcia. A comprehensive survey on safe reinforcement learning. *Journal of Machine Learning Research*, 16:1437–1480, 2013.
- [13] I. Kolmanovsky and E.G. Gilbert. Theory and computation of disturbance invariant sets for discrete-time linear systems. *Math. Probl. Eng.*, 4(4):317–367, 1998.
- [14] David Q. Mayne. Model predictive control: Recent developments and future promise. *Automatica*, 50(12):2967 – 2986, 2014.
- [15] J. Nocedal and S.J. Wright. *Numerical Optimization*. Springer Series in Operations Research and Financial Engineering. Springer, 2 edition, 2006.
- [16] P. O. M. Scokaert and D. Q. Mayne. Min-max feedback model predictive control for constrained linear systems. *IEEE Transactions on Automatic Control*, 43:1136–1142, 1998.
- [17] David Silver, Guy Lever, Nicolas Heess, Thomas Degris, Daan Wierstra, and Martin Riedmiller. Deterministic policy gradient algorithms. In *Proceedings of the 31st International Conference on Machine Learning, ICML’14*, pages I–387–I–395, 2014.
- [18] Richard S. Sutton and Andrew G. Barto. *Introduction to Reinforcement Learning*. MIT Press, Cambridge, MA, USA, 1st edition, 1998.
- [19] Richard S. Sutton, David McAllester, Satinder Singh, and Yishay Mansour. Policy gradient methods for reinforcement learning with function approximation. In *Proceedings of the 12th International Conference on Neural Information Processing Systems, NIPS’99*, pages 1057–1063, Cambridge, MA, USA, 1999. MIT Press.
- [20] Shouyi Wang, Wanpracha Chaovalitwongse, and Robert Babuska. Machine learning algorithms in bipedal robot control. *Trans. Sys. Man Cyber Part C*, 42(5):728–743, September 2012.
- [21] M. Zanon and Gros. Safe Reinforcement Learning Using Robust MPC. In *Transaction on Automatic Control, Archivx*, 2019. (submitted).



Sébastien Gros received his Ph.D degree from EPFL, Switzerland, in 2007. After a journey by bicycle from Switzerland to the Everest base camp in full autonomy, he joined a R&D group hosted at Strathclyde University focusing on wind turbine control. In 2011, he joined the university of KU Leuven, where his main research focus was on optimal control and fast NMPC for complex mechanical systems. He joined the Department of Signals and Systems at Chalmers University of Technology, Göteborg in 2013, where he became associate Prof.

in 2017. He is now full Prof. at NTNU, Norway and guest Prof. at Chalmers. His main research interests include numerical methods, real-time optimal control, reinforcement learning, and energy-related applications.



Mario Zanon received the Master's degree in Mechatronics from the University of Trento, and the Diplôme d'Ingénieur from the Ecole Centrale Paris, in 2010. After research stays at the KU Leuven, University of Bayreuth, Chalmers University, and the University of Freiburg he received the Ph.D. degree in Electrical Engineering from the KU Leuven in November 2015. He held a Post-Doc researcher position at Chalmers University until the end of 2017 and is now Assistant Professor at the IMT School for Advanced Studies Lucca. His research interests

include numerical methods for optimization, economic MPC, optimal control and estimation of nonlinear dynamic systems, in particular for aerospace and automotive applications.